Published in final edited form as:
Inorg Chem. 2010 March 1; 49(5): 2398–2406. doi:10.1021/ic902309f.

Oxygenation of Cobalt Porphyrinates: Coordination or Oxidation?

Jianfeng Li, **Bruce C. Noll**, **Allen G. Oliver**, **Guillermo Ferraudi**, **A. Graham Lappin***, and **W. Robert Scheidt***
Department of Chemistry and Biochemistry, University of Notre Dame, Notre Dame, Indiana 46556

Abstract

The X-ray characterization of the five-coordinate picket-fence porphyrin complex, [Co(TpivPP)(2-MeHim)], is reported. The complex has the displacement of cobalt from the porphyrin plane = 0.15 Å, and Co–N_{Im} = 2.145 (3) and (Co–N_p)$_{av}$ = 1.979(3) Å. This five-coordinate complex, in the presence of dioxygen and excess 2-methylimidazole, undergoes an unanticipated, photoinitiated atropisomerization of the porphyrin ligand, oxidation of cobalt(II) and the formation of the neutral cobalt(III) complex [Co(*α*,*α*,*β*,*β*-TpivPP)(2-MeHim)(2-MeIm$^-$]. Two distinct examples of this complex have been structurally characterized, both have structural parameters consistent with cobalt (III). The two new Co(III) porphyrin complexes have axial Co–N_{Im} distances ranging from 1.952 to 1.972 Å, but which allow for the distinction between imidazole and imidazolate. An interesting intermolecular hydrogen bonding network is observed that leads to infinite helical chains. UV-vis spectroscopic study suggests that [Co(TpivPP)(2-MeHIm)(O_2)] is an intermediate state for the oxidation reaction and the atropisomerization process is photocatalyzed. A reaction route is proposed based on the spectroscopic studies.

Introduction

The interaction of cobalt complexes with dioxygen to form species with coordinated dioxygen have been known for some time; both reversible and irreversible dioxygen binding have been reported.[1, 2] Similarly, five-coordinate cobalt(II) porphyrinates show reversible binding of dioxygen.[3] Cobalt myoglobin and cobalt hemoglobin, “coboglobin”, in which the heme prosthetic group (iron protoporphyrin IX) is replaced by cobalt protoporphyrin IX display reversible oxygen binding similar to those of their native iron counterparts.[4] These species have been the subject of interest for many years in regard to the nature of the bond between cobalt and oxygen in the monomeric oxygen adducts.[2] The reactions required for understanding the O_2 interactions with cobalt porphyrinates, [Co(Por)(L)],[5] are shown below.[3]

$$\mathrm{Co\,(Por)} \quad + \quad \mathrm{L} \quad \overset{K_1}{\rightleftharpoons} \quad \mathrm{[Co\,(Por)\,(L)]} \tag{1}$$

*To whom correspondence should be addressed: WRS: Scheidt.1@nd.edu, Fax, (574) 631-6652, AGL: Alexander.G.Lappin.1@nd.edu.

Supporting Information Available: Figures S1, S4 and S5 giving 24-atom mean plane drawings for [Co(TpivPP)(2-MeHIm)], [Co(*α*,*α*,*β*,*β*-TpivPP)(2-MeHIm)(2-MeIm$^-$)] (monoclinic) and [Co(*α*,*α*,*β*,*β*-TpivPP)(2-MeHIm)(2-MeIm$^-$)] (triclinic). Figures S2 and S3 giving ORTEP diagrams for [Co(*α*,*α*,*β*,*β*-TpivPP)(2-MeHIm)(2-MeIm$^-$)] (triclinic). Figure S6 giving packing diagram of complex [Co(*α*,*α*,*β*,*β*-TpivPP)(2-MeHIm)(2-MeIm$^-$)] (triclinic) showing the unit cell and the hydrogen bonds between the axial ligands. Figure S7 giving selected UV-vis spectra taken in benzene. Figure S8 giving oscillographic traces recorded at 450 and 525 nm. Tables S1–S18 giving complete crystallographic details, atomic coordinates, bond distances and angles, anisotropic temperature factors, and fixed hydrogen atom positions for [Co(TpivPP)(2-MeIm)], [Co(*α*,*α*,*β*,*β*-TpivPP)(2-MeHIm)(2-MeIm$^-$)] (monoclinic) and [Co(*α*,*α*,*β*,*β*-TpivPP)(2-MeHIm)(2-MeIm$^-$)] (triclinic). X-ray crystallographic information (CIF). This material is available free of charge via the Internet at http://pubs.acs.org.

$$[\mathrm{Co(Por)(L)}] + \mathrm{L} \overset{K_2}{\rightleftharpoons} [\mathrm{Co(Por)(L)_2}] \quad (2)$$

$$[\mathrm{Co(Por)(L)}] + \mathrm{O_2} \rightleftharpoons [\mathrm{Co(Por)(L)(O_2)}] \quad (3)$$

$$[\mathrm{Co(Por)(L)}] + [\mathrm{Co(Por)(L)(O_2)}] \rightleftharpoons [\mathrm{(L)(Por)Co(O_2)Co(Por)(L)}] \quad (4)$$

Some features of these reactions are noteworthy. First, the binding of nitrogen ligands (L) to form six-coordinate [Co(II)(Por)$(L)_2$] is extremely unfavorable at room temperature (reaction 2), which is the result of the destabilization of the six-coordinate complex by the singly populated d_z2 orbital.[6, 7] For example, in toluene this binding takes place only at very high ligand concentrations (with piperidine, a ~10^5-fold ligand excess is required).[6, 7] It is perhaps not surprising that no bis(imidazole)-ligated Co(II) porphyrinate has ever been isolated. Second, a number of Co(II) porphyrins can form 1:1 mononuclear oxygen adducts that are generally reversible (reaction 3).[3, 8] Third, both reversible and irreversible reactions have been reported for forming the 1:2 peroxo-bridged binuclear complexes [(L)(Por)Co(O_2)Co(Por)(L)] (reaction 4). For example, in a carefully purified toluene solution the decreased EPR signal due to formation of [(L)(Por)Co(O_2)Co(Por)(L)] could be restored by heating or pumping off dioxygen to decompose the diamagnetic binuclear products.[3] However, under some conditions an irreversible reaction takes place. Yamamoto and coworkers concluded that oxygen-bridged complexes were formed in an irreversible manner from cobalt tetraphenylporphyrin when L was imidazole or benzimidazole after oxygenation at room temperature; reactions in the presence of other amines were reversible.[9]

It is also important to note that the oxygen reduction catalyzed by porphyrins has been of great interest in fields as diverse as biology, photosynthesis, and electrocatalysis.[10] For instance, cobalt porphyrin complexes have been shown to catalyze the four-electron reduction of O_2 to H_2O (reaction 5) when adsorbed on graphite electrodes,[11] and to mainly catalyze the two-electron reduction of O_2 to yield hydrogen peroxide (H_2O_2) (reaction 6) when deposited onto gold electrodes.[12]

$$\mathrm{O_2} + 4\mathrm{H^+} + 4\mathrm{e^-} \rightarrow 2\mathrm{H_2O} \quad (5)$$

$$\mathrm{O_2} + 2\mathrm{H^+} + 2\mathrm{e^-} \rightarrow \mathrm{H_2O_2} \quad (6)$$

As part of our study of the vibrational and dynamical characterization of dioxygen complexes of cobalt and iron porphyrinates we report in this paper the reactions of cobalt picket fence porphyrin with 2-methylimidazole and dioxygen. Although the reaction with 2-methylimidazole and the four-coordinate cobalt derivative proceeded as expected to yield the five-coordinate species, the further reactions of this product and dioxygen led to interesting new six-coordinate cobalt(III) products. We report the molecular structures of both the five-coordinate complex, [Co(TpivPP)(2-MeHIm)] and the six-coordinate species, [Co(TpivPP′)(2-MeHIm)(2-$MeIm^-$)]. Interestingly, the picket fence porphyrin is atropisomerized during the oxidation reaction to produce new six-coordinate species. The atropisomerization of the porphyrin ligand occurs even though all reactions were carried out at ambient temperature. The

atropisomerization process appears to be photocatalyzed and we have investigated the reaction via flash photolysis experiments.

Experimental Section

General Information

All reactions and manipulations were carried out under argon using a double-manifold vacuum line, Schlenkware and cannula techniques. Benzene, THF and heptane were distilled over sodium/benzophenone and ethanol over magnesium. Research grade oxygen (99.999%) was purchased from PRAXAIR and used as received. [H_2(TpivPP)] and [Co(TpivPP)] were prepared according to a local modification of the reported syntheses.[8b,13] UV-vis spectra were recorded on a Perkin-Elmer Lambda 19 UV/vis/near-IR spectrometer.

Synthesis of [Co(II)(TpivPP)(2-MeHIm)]

[Co(II)(TpivPP)] (10.1 mg, 9.5 mmol) was dried in vacuum for 30 mins and dissolved in 2.5 mL benzene to give a clear dark red solution. This solution was added to 2-methylimidazole (4.1 mg, 49.9 mmol) and 8 drops of ethanol by cannula. The mixture was stirred for 20 mins and transferred into 8 mm × 250 mm glass tubes which were layered with heptane as nonsolvent. The tubes were kept in a 5°C refrigerator and X-ray quality crystals were obtained after two weeks.

[Co(III)(TpivPP′)(2-MeHIm)(2-MeIm⁻)]

[Co(II)(TpivPP)] (8.6 mg, 8.1 mmol) was dried in vacuum for 30 mins and dissolved in 2 mL benzene. This solution was transferred to 2-methylimidazole (9.7 mg, 118.2 mmol) and 8 drops of ethanol by cannula. Oxygen was then bubbled into the mixture for 3 mins. X-ray quality crystals were obtained in 8 mm × 250 mm sealed glass tubes by liquid diffusion using heptane as nonsolvent. Two crystalline forms have been isolated that crystallize in the triclinic or monoclinic crystal systems. The two differ only in the benzene solvent content.

Equilibrium Constant Determinations

UV-vis spectra were recorded on a Perkin-Elmer Lambda 19 UV/vis/near-IR spectrometer in a specially designed combined 1- and 10-mm inert atmosphere cell. A solution of the four-coordinate Co(II) porphyrin was prepared using benzene as solvent. The ligand solution was prepared by dissolving 2-methylimidazole in EtOH and the concentrations for UV-vis measurements is 0.06 M. The 2-MeHIm solution was titrated into [Co(II)(TpivPP)] solution. UV-vis spectra of [Co(II)(TpivPP)] in different concentrations of 2-MeHIm were measured. The equilibrium constant for the equilibria was calculated with the nonlinear least-squares program SQUAD.[14] SQUAD calculates best values for the equilibrium constants by employing multiple-wavelength absorption data for varying concentrations of the reactants. Absorbance data, at 10-nm increments spanning the visible region, were input into SQUAD. The calculated results are $K_1 = 3.5 \pm 0.5 \times 10^4\ M^{-1}$.

$$\mathrm{Co\,(TpivPP)} \quad + \quad \mathrm{2-MeHIm} \quad \overset{K_1}{\rightleftharpoons} \quad \mathrm{Co\,(TpivPP)\,(2-MeHIm)} \tag{1}$$

X-ray Structure Determinations

Single-crystal experiments were carried out on a Bruker Apex system with graphite-monochromated Mo Kα radiation (λ = 0.71073 Å). The structures were solved by direct methods using SHELXS-97[15] and refined against F^2 using SHELXL-97;[16, 17] subsequent difference Fourier syntheses led to the location of most of the remaining nonhydrogen atoms.

For the structure refinement all data were used including negative intensities. All nonhydrogen atoms were refined anisotropically if not remarked otherwise below. Except as noted below, hydrogen atoms were idealized with the standard SHELXL-97 idealization methods. The program SADABS[18] was used to apply an absorption correction. A brief summary of the crystallographic data is given in Table 1. Complete crystallographic details, atomic coordinates, anisotropic thermal parameters, and fixed hydrogen atom coordinates are given in the Supporting Information for the three structures.

[Co(TpivPP)(2-MeIm)]·2C_2H_5OH

A black crystal with the dimensions 0.50 × 0.22 × 0.21 mm^3 was used for the structure determination. In this structure, the asymmetric unit contains a half picket fence porphyrin complex, and two half-ethanol solvent molecules. There is a crystallographic twofold axis passing through the cobalt atom. The 2-methylimidazole ligand was found to disorder between two twofold related sites. Each solvent ethanol molecule also possesses a twofold axis.

[Co(TpivPP′)(2-MeHIm)(2-MeIm⁻)](monoclinic)

A black crystal with the dimensions 0.49 × 0.20 × 0.12 mm^3 was used for the structure determination. The asymmetric unit contains one six-coordinate picket fence porphyrin complex, and 2.65 benzene solvent molecules. The two axial ligands are found to be completely ordered. The hydrogen atoms were located and refined in two steps. In the first step all the hydrogen atoms, except those on the five-membered imidazole (or imidazolate) ring of the two axial ligands, are located either in the Fourier maps or by calculation. In the second step, the hydrogen atoms on the five-membered imidazole (or imidazolate) ring of the two axial ligands are carefully located from the Fourier maps. Hydrogen atoms for all imidazole or imidazolate ligands were located except that for N8. Thus the axial ligand of N7–C5–N8–C6–C7–C8 is determined as the 2-methylimidazolate ligand. In order to verify the hydrogen atom assignment of the imidazole and imidazolate ligands, these hydrogen atoms were refined in the least square processes allowing both coordinates and isotropic temperature factors to vary. Refined C–H distances range from 0.84 to 1.13 Å, N–H distances range from 0.73 to 0.94 , and temperature factors for all hydrogen atoms range from 0.02 to 0.09.

[Co(TpivPP′)(2-MeHIm)(2-MeIm⁻)](triclinic)

A black crystal with the dimensions 0.40 × 0.32 × 0.12 mm^3 was used for the structure determination. The asymmetric unit contains two six-coordinate picket fence porphyrin complexes, and 2.35 benzene solvent molecules. In the first porphyrin complex (Co1), on one of the “pickets”, the pivalamido methyl carbon atoms are found to disorder into two sets of positions. An ideal tetrahedral group[19] is applied as rigid group to constrain each *tert*-butyl group. The occupancies of two pairs of *tert*-butyl groups are refined to be 0.732(9) and 0.268 (9). The remaining three “pickets” are ordered. The second porphyrin complex (Co2) is more disordered. For the first “picket”, the whole pivalamido group and the attached phenyl group are disordered into two sets of positions. For the second “picket”, both the pivalamido methyl carbons and the carbonyl group are disordered into two sets of positions. For the third “picket”, the pivalamido methyl carbons are disordered into two sets of positions. For each pair of these disordered moieties, the occupancy factors of are refined by means of “free variables”. The fourth “picket” is ordered. The two axial ligands (2-methylimidazole and 2-methylimidazolate) on each of the porphyrin complex are found to be completely ordered. The hydrogen atoms are located and refined in two steps. In the first step, all the hydrogen atoms, except those on the five-membered imidazole (or imidazolate) ring of the four axial ligands, are located by calculations. In the second step, the hydrogen atoms on the five-membered imidazole (or imidazolate) ring of the four axial ligands are carefully found from the Fourier maps. It was found that all the hydrogen atoms were located except those for N16 and N28. Thus the axial

ligand of N15–C1–N16–C2–C3–C4 and N27–C13–N28–C14–C15–C16 are determined as the 2-methylimidazolate ligands. In order to verify the hydrogen atom assignment of the imidazole and imidazolate ligands, these hydrogen atoms were refined in the least square processes allowing both coordinates and isotropic temperature factors to vary.

Photochemical Procedures

Absorbance changes, ΔA, occurring in a time scale longer than 10 ns were investigated at room temperature with a flash photolysis apparatus described elsewhere.[20] In these experiments, 10 ns flashes of 351 nm light were generated with a Lambda Physik SLL-200 excimer laser. The energy of the laser flash was attenuated to values equal to or less than 20 mJ/pulse. A right angle configuration was used for the pump and the probe beams. Concentrations of the chromophores in the solution were adjusted to provide homogeneous concentrations of photogenerated intermediates over the 1 cm optical path of the probe beam. Both carefully degassed solutions and solutions saturated with O_2 or air were used in the photochemical experiments.

The reaction kinetics was investigated by following the absorbance change at given wavelengths of the spectrum and incorporating those changes in

$$\rho = (\Delta A_{inf} - \Delta A_t) / (\Delta A_{inf} - \Delta A_0) .$$

[21] In the expression of the dimensionless parameter ρ, ΔA_0 is the absorbance change at the beginning of the reaction, ΔA_t is determined at an instant t of the reaction and ΔA_{inf} is determined at the end of the reaction. Values of ρ were fitted to the integrated rate law by a nonlinear least-squares method.

Results and Discussion

Structures

We have been investigating the vibrational spectroscopy of dioxygen complexes of iron porphyrinates with the technique of nuclear resonance vibration spectroscopy (NRVS).[22] Interesting crystallographic difficulties for several six-coordinate dioxygen complexes of iron in those studies have led us to the examination of the interaction of dioxygen with cobalt(II) porphyrinates. One of the systems we have studied is that of the cobalt(II) picket fence porphyrin derivative with the hindered imidazole 2-methylimidazole. The use of hindered imidazoles is a necessary condition to prepare five-coordinate iron(II) species, but this is not apparently necessary for cobalt(II) species. Indeed, to our knowledge only five-coordinate derivatives result from the reaction of four-coordinate cobalt(II) porphyrin derivatives with any imidazole derivative. Thus the preparation, crystallization, and structure determination of [Co(II)(TpivPP)(2-MeHIm)] proceeded smoothly; the structure is displayed in Figure 1.

The structural parameters of [Co(II)(TpivPP)(2-MeHIm)] can be compared with those previously observed on five-coordinate imidazole-ligated cobalt(II) and iron(II) derivatives given in Table 2. The significant differences between the cobalt(II) and iron(II) derivatives are the consequence of the differing spin states. All cobalt(II) derivatives have a low-spin d electron configuration of $(d_{xy},d_{xz},d_{yz})^6 (d_{z^2})^1$ whereas iron(II) derivatives have a high-spin d electron configuration of $(d_{xz})^2(d_{yz},d_{xy})^2(d_{z^2})^1(d_{x^2-y^2})^1$. These electronic state properties lead to the large differences in the metal out-of-plane displacements and the much larger in-plane M–N_p bond distance values for iron.

The structural parameters of [Co(II)(TpivPP)(2-MeHIm)] have very similar values to those of the other cobalt(II) derivatives given in Table 2. The axial Co–N_{Im} bond distance of 2.145 (3)

Å to the hindered imidazole is similar to those found in the unhindered derivatives, rather than somewhat larger owing to the increased steric hindrance (cf. the 2.216-Å value found for [Co(TPP)(1,2-Me_2Im)]). Hoard and Scheidt had suggested that the axial Co–N_{im} bond in the five-coordinate porphinato complexes should be readily stretched by reason of the presence of the odd electron in the d_{z^2} orbital of the metal atom.[31] However, we note that a similar, shorter than expected, axial distance to the hindered imidazole is also seen in the analogous iron(II) picket fence derivative (Table 2). We are unable to say whether this is a specific effect of picket fence porphyrin. The porphyrin core of [Co(II)(TpivPP)(2-MeHIm)] shows a modest saddling behavior consistent with the required twofold symmetry. A formal diagram along with averaged values of the bond distances and angles in the core is given in Figure S1.

Five-coordinate [Co(II)(TpivPP)(2-MeHIm)] had been prepared in order to prepare and characterize the six-coordinate dioxygen complex [Co(II)(TpivPP)(2-MeHIm)O_2]. The reaction of O_2 with the crystalline five-coordinate cobalt(II) complex under the same conditions as that used previously for the five-coordinate iron(II)[27] leads only to an modestly (partially) oxygenated complex. This result is comparable to the solid state oxygenation of the B_{12} derivative Co(II)alamin, the product of which reaction contains about 30% of the unoxygenated speices.[32] A completely oxygenated porphyrin species can be prepared, the conditions and results are still under study. They will be reported along with the characterization of other (more traditional) oxygenated cobalt species.[33]

The direct reaction of a benzene solution [Co(II)(TpivPP)(2-MeHIm)] with dioxygen yielded an unanticipated product rather than a crystalline dioxygen complex. In the course of carrying out these reactions we have obtained the same compound in two different forms. The two crystalline systems contained a total of three unique cobalt centers, all three are essentially equivalent. Figure 2 displays a thermal ellipsoid plot of one of the centers. There are several striking features. First, the pickets of the picket fence porphyrin have atropisomerized from the *α*, *α*, *α*, *α* conformation (all up) to an *α*, *α*, *β*, *β* conformation. This atropisomerization has occurred even though the reaction solutions were never heated above ambient temperature. Illustrations of the other two characterized cobalt centers in the triclinic crystalline form are given as Figures S2 and S3. These centers have also undergone atropisomerization to the *α*, *α*, *β*, *β* conformer.

The other striking feature of all three cobalt centers is the six-coordinate structure with two imidazole ligands. The two axial Co–N bonds at all three centers are both very short at 1.95–1.97 Å. As shown in Table 3, such short bonds are inconsistent with the cobalt center having a +2 oxidation state, but are consistent with a +3 oxidation state. We can thus conclude the cobalt must have been oxidized upon oxygenation. Other structural features are also consistent with oxidation of the cobalt centers. The coordination of two imidazole ligands to a cobalt(II) center would be unprecedented. As is clearly evident in the illustration of Figure 2, the porphyrin core is severely ruffled. This severe ruffling, quantitatively illustrated in Figures S4 and S5, leads to very short equatorial bonds. The two new Co(III) structures have the shortest $(Co–N_p)_{av}$ distances (1.934(5), 1.943(5) and 1.951(4) Å) among the complexes of Table 3. As is well-known, core ruffling and short M–N_p bonds are tightly coupled parameters, with core ruffling leading to shortened M–N_p bonds.[38, 39] The ruffling also accommodates the two sterically hindered axial ligands with their demanding 2-methyl group in relative perpendicular orientations; the dihedral angles are 71.2, 80.2 and 85.° (Table 3).

An oxidation of the cobalt ion would require the presence of an anion. In both crystalline complexes this anion is provided by the deprotonation of one of the two axial imidazoles so that the axial ligands to the cobalt in both crystalline forms consists of one imidazole and one imidazolate ligand. Moreover, a careful examination of the crystal packing and final difference Fourier syntheses are strongly consistent with the identification and complete ordering of the

axial ligands. The imidazolate ligand of one cobalt center is hydrogen bonded to the imidazole ligand of the next molecule so as to form an infinite one-dimensional chain and which can be formulated as ···Co–2-MeIm$^-$···H–2-MeIm–Co···. A packing diagram of a portion of the cell of the monoclinic form of [Co(*α*,*α*,*β*,*β*-TpivPP)(2-MeHIm)(2-MeIm$^-$)] is shown in Figure 3; an analogous diagram for the triclinic form is given in Figure S6. In all cases, the ligand identified by the X-ray analysis as the imidazolate has the shorter axial Co–N bond (see Table 3); however, the difference in one case is not statistically significant.

The hydrogen bonds found in the two new structures are relatively strong with N···N distances of 2.662(5), 2.636(5), and 2.667(5) Å. These studies would suggest that an atropisomerization for a metal complex will have a fairly high activation barrier. These distances are much shorter than the mean value of 2.900 Å, found for a total of 391 instances from the Cambridge Structural Database[40] of a hydrogen bond formed by an imidazole derivative to a nitrogen atom acceptor in a solid-state structure.[41] Moreover, some structural differences derived from the two different axial ligands (2-MeHIm and 2-MeIm$^-$) are expected and readily observed. First, the bond distances and angles involving the two nitrogen atoms are expected to be more similar in imidazolate than in imidazole due to the increased bond delocalization for the imidazolate ring. In [Co(*α*,*α*,*β*,*β*-TpivPP)(2-MeHIm)(2-MeIm$^-$)](monoclinic), for example, the angles around the two nitrogen atoms are 105.5(3) and 105.2(3)° for 2-MeIm$^-$ and 105.4(3) and 108.4 (4)° for 2-MeHIm. Second, the imidazolate ligand is known to be a stronger field ligand than imidazole and is also expected to be a better *σ* donor;[42] that these effects lead to an ~0.02 axial Co–N bond distance shortening in [Co(*α*,*α*,*β*,*β*-TpivPP)(2-MeHIm)(2-MeIm$^-$)](monoclinic).

It is to be presumed that formation of the hydrogen-bonded chain is much more favorable with the atropisomerized porphyrin ligand compared to the *α*, *α*, *α*, *α* conformer. The issue of which particular atropisomer is formed is an interesting question. The perpendicular orientation of the two axial ligands would, at first glance suggest that the most likely atropisomer would be the *α*,*β*,*α*,*β* form. However, the *α*, *α*, *β*, *β* conformer would appear to better allow the close contacts the hydrogen-bonded five-membered rings require. The hydrogen-bonded chains are helical; the space group requirements do however require that both helical hands are present. We had originally thought that the *α*, *α*, *β*, *β* conformer resulted from a concerted process in which a binuclear intermediate was important, but the photolysis experiments (vide supra) do not suggest such an intermediate.

A few studies on the atropisomerization of picket fence porphyrin complexes have been reported.[43, 44] The process would seem to have a relatively high activation barrier. Atropisomerism of any metal complex of a picket fence porphyrin will almost certainly require ruffling of the porphyrin core in order to increase the distance between the ortho substituent and the pyrrole hydrogens, thereby reducing the interaction responsible for restricted phenyl ring rotation.[43] Thus, a cobalt(III) complex with the generally observed strong ruffling is a reasonable system for atropisomerization. However, no atropisomerized structures of a picket fence complex has been reported. Marchon and coworkers have reported the occurrence of atropisomerism in another “pocketed” porphyrin system, the chiroporphyrins, that responded to changes in complexation.[45] The apparently facile atropisomerization of the cobalt picket fence derivative suggests that this feature is deeply involved in the mechanism of the reaction of the cobalt(II) complex with dioxygen. In particular this suggests the possibility of a binuclear O_2 bridged intermediate. This possibility led us to carefully study the solution reaction chemistry of these systems.

Reactions

We have monitored the reaction of [Co(II)(TpivPP)] with 2-methylimidazole in both the presence and absence of oxygen. In the absence of oxygen, the titration of a benzene solution of [Co(II)(TpivPP)] with ethanol solutions of 2-MeHIm gave the results shown in Figure 4.

The Soret and α bands decrease in intensity and shift very slightly to longer wavelength as the concentration of ligand is increased from $2.40 \times 10^{-}5$ M to $1.06 \times 10^{-}3$ M. The results are consistent with previously reported results[46] and suggests only the five-coordinate complex is formed (reaction 1). No evidence for the formation of a bis(imidazole) complex (reaction 2), even at higher concentrations of imidazole than those shown in Figure 4, was observed.

When the reaction system was exposed to air, a decrease of the Soret band at 411 nm and the simultaneous appearance of a new Soret band at ~445 nm was observed. In the visible region, the band at 529 nm was gradually replaced by one at 561 nm (Figure 5). The appearance of the new, 34 nm, blue-shifted Soret band strongly indicates the oxidation of Co(II) to Co(III).[47] These initial reactions were carried out with an ethanolic solution of 2-MeHIm. Similar spectral changes are observed when the reactions were run in the absence of ethanol. These spectral changes are consistent with formation of [Co(III)(α,α,β,β-TpivPP)(2-MeHIm)(2-MeIm^{-})] we described above.

Further insight into the processes were given by additional spectral measurements. In a carefully purified benzene solution of [Co(II)(TpivPP)] (ethanol-free), excess solid 2-MeHIm was added and dissolved. Then oxygen gas was introduced for 3 minutes. The immediately recorded UV-vis spectra showed a decrease of the Soret band at 411 nm and the appearance of a shoulder at ~439 nm (Figure 6). Simultaneously in the visible, the band at 529 nm moved to 549 nm. The reported spectral observation of oxygen bonding for [Co(TpivPP)(1-MeIm)] and [Co(TpivPP)(1,2-Me_2Im)] are the shifts of λ_{max} from 530 to 547 nm and from 529 to 546 nm, respectively.[8b] This is consistent with our observations and indicates formation of the oxygen adduct of [Co(TpivPP)(2-MeHIm)(O_2)]. This reversible reaction (Reaction 3) was confirmed by an argon purge of the reaction solution that led to an immediate diminishing of the shoulder at ~ 439 nm and the return of λ_{max} from 549 to 529 nm. Importantly, the best results were obtained when the processes were carried out in subdued light. Conversely, if the argon purge was not done and the solution was then stirred continuously under ambient light, the shoulder at ~439 nm gradually shifts to 445 nm with a decrease of the band at 411 nm. This behavior, consistent with the formation of Co(III), is irreversible and unaffected by an argon purge. If the solution of the cobalt complex, imidazole, and O_2 is stirred overnight in the dark, only slight changes in the spectra are observed.

Two conclusions from these spectral observations can be drawn: 1) the first product of the oxygenation reaction is the oxygen adduct [Co(TpivPP)(2-MeHIm)(O_2)] and 2) the oxidation reaction (Co(II) → Co(III)) can proceed without a proton source other than 2-methylimidazole. There are a number of possibilities (and questions) in the reaction sequence between the formation of the monomeric oxygen complex and the final cobalt(III) product. Clearly the porphyrin ligand must be atropisomerized, but what is the driving force for the atropisomerization of picket fence porphyrin when all the reactions are at room temperature? Normally picket fence porphyrin is stable to atropisomerization at room temperature.[13] Protons are required if O_2 is the oxidant and must be provided by the 2-methylimidazole, which then becomes the second ligand of the final oxidized product. Does this imply that a binuclear oxygen-bridged species, (L)(Por)Co(O_2)Co(Por)(L), is an important species as suggested by James et al.[47] or is only a monomeric reactive O_2 complex involved as suggested by Asperger et al.[48] The importance of a light-induced process in taking the reaction further led us to explore the photochemical behavior of this system.

The photochemical behavior of [Co(TpivPP)] was investigated by nanosecond flash photolysis in benzene solution, irradiating at 351 nm. The complex in the presence and absence of 2-MeHIm showed no significant evidence for the formation of any transient species. Admission of O_2 to the system results in the formation of the O_2 bound complex, [Co(TpivPP)(2-MeHIm)(O_2)], that ultimately yields the product [Co(TpivPP)(2-MeHIm)(2-MeIm^{-})]. The initial

photochemical process shows formation of a transient with a lifetime in the microsecond range, Figure 7. When observed at wavelengths where the absorption of the ultimate reaction product does not interfere, the transient decays back to the starting complex by second-order kinetics indicating that the transient is most likely Co^{δ}+(TpivPP)(2-MeHIm)$(O_2)^{\delta-}$···H···2-MeIm. At 450 nm, a wavelength where the product formation reaction is observed, the process is first order and independent of 2-MeHIm, with a rate constant of 5×10^6 s^{-1}. (See Figure S8.) Experimental difficulties prevent the determination of the Soret maximum of this initial product but it has absorption characteristics similar to the final reaction product. It is likely that the rate limiting/determining step in this instance corresponds to the inversion/rotation of the ortho-substituted "picket fence" groups. Although thermally induced atropisomerization of picket fence porphyrins is slow,[43] the values obtained herein are consistent with the photo-catalyzed process reported for the free ligand by Whitten.[43] Indeed, when coordinated to a small cation such as cobalt(III), further acceleration can be expected as the porphyrin is subject to out-of-plane distortions.

The photochemical study supports a photoinitiated transient state that involves the atropisomerization of picket fence porphyrin. Based on the experimental observations and analysis, we propose the following reaction scheme for the formation of [Co(III)(*α*,*α*,*β*,*β*-TpivPP)(2-MeHIm)(2-MeIm$^-$)] starting from five-coordinate [Co(TpivPP)(2-MeHIm)] (Scheme 1). [Co(TpivPP)(2-MeHIm)(O_2)] is the first reaction product, and whose formation is reversible. In the presence of excess 2-MeHIm and O_2, a transient state is initiated by photolysis. In this transient state, both the steric effect from bulky 2-MeHIm ligand and the photo energy are presumed to be the driving force for the atropisomerization of picket fence porphyrins. With the release of $HO_2^{\bullet}$, the final product of [Co(III)(*α*,*α*,*β*,*β*-TpivPP)(2-MeHIm)(2-MeIm$^-$)] is produced.

Finally, we emphasize the importance of the hydrogen bond between $Co^{\delta+}$(Por)(L)$(O_2)^{\delta-}$ and the hydrogen bond donor (2-methylimidazole in this study) in the oxygenation/oxidation reactions. The presence of a hydrogen bond donor to the coordinated dioxygen ligand appears crucial to the question of whether reversible oxygenation or oxidation occurs. As noted in the Introduction, both reversible and irreversible reactions had been claimed for forming the binuclear complex (L)(Por)Co(O_2)Co(Por)(L) (reaction 4).[9] In this report irreversible reactions were reported for two imidazole ligands with an acidic hydrogen (*e.g.* imidazole and the 1-position NH for benzimidazole); none of the ligands reported as having reversible oxygenation behavior had acidic protons. James and coworkers had suggested the importance of imidazole hydrogen bonding in Co(Por)(L)···O_2···H···Im, which was believed to lower the transition state by ~4 Kcal mol^{-1}, giving products of (L)(Por)Co(O_2)Co(Por)(L) or Co(Por)(L)(OH).[47] Definitive characterization of products in these reactions is not available.

In other reported cases, the solvent provides the hydrogen bonding donor. The formation of $L_5C_oO_2CoL_5$ (L is nitrogenous bases) in water was reported to be very rapid and difficult to reverse.[49] In alcoholic media as the proton source the oxidation of [Co(II)(Por)(L)] to [Co(III)(Por)(L_2)]$^+$ is reported.[48] In the reversible case reported by Walker, the carefully purified toluene solution excluded water and the EPR signal can be restored by pumping off the dioxygen.[3] In our system, the combination of the protecting "picket fence" and the bulky 2-methylimidazole would appear to preclude the formation of the peroxo-bridged binuclear complex but could allow hydrogen bonding to the O_2 by excess 2-methylimidazole. It is thus possible that a preorganized hydrogen-bonded (TpivPP)Co–O_2 ···H-2-MeHIm ensemble is ready for the photoinitiated atropisomerism followed by oxidation of cobalt and coordination of the resulting imidazolate ligand.

Summary

The synthesis and structural characterization of the five-coordinate complex [Co(TpivPP)(2-MeHIm)] is reported. The reaction of this species in the presence of dioxygen and light to yield a novel cobalt(III) complex coordinated by imidazole and imidazolate has been studied by structural analysis and flash photolysis. Amongst other surprising features, these reaction conditions lead to the atropisomerization of the picket fence porphyrin from the usual α, α, α, α conformer to the α, α, β, β conformer with the two axial ligands having relative perpendicular orientation. The atropisomerism occurs under very mild conditions and appears to be photoinitiated.

Supplementary Material

Refer to Web version on PubMed Central for supplementary material.

Acknowledgments

We thank the National Institutes of Health for support of this research under Grant GM-38401 and the NSF for X-ray instrumentation support under Grant CHE-0443233.

References and Notes

1. Niederhoffer EC, Timmons JH, Martell AE. Chem. Rev 1984;84:137.
2. Jones RD, Summerville DA, Basolo F. Chem. Rev 1979;79:139.
3. (a) Walker FA. J. Am. Chem. Soc 1970;92:4235. (b) Walker FA. J. Am. Chem. Soc 1973;95:1154. [PubMed: 4347146]
4. (a) Hoffman BM, Petering DH. Proc. Natl. Acad. Sci. U.S.A 1970;67:637. [PubMed: 4331717] (b) Chien JCW, Dickinson LC. Proc. Natl. Acad. Sci. U.S.A 1972;69:2783. [PubMed: 4342964]
5. Abbreviations: Por, generalized porphyrin dianion; N_p, porphyrinato nitrogen; N_{Ax}, nitrogen of axial ligands; N_{im}, nitrogen of imidazole ligands; L_{sixth}, the sixth ligand of the porphyrin complex; Δ_{24}: displacement of metal atom from the 24-atom mean plane; EPR, electron paramagnetic resonance. Mb, Myoglobin; TpivPP, dianion of *α*,*α*,*α*,*α*-tetrakis(*o*-pivalamidophenyl)porphyrin; TpivPP′, dianion of *α*,*α*,*β*,*β*-tetrakis(*o*-pivalamidophenyl)porphyrin; RIm, generalized imidazole; 1-MeIm, 1-methylimidazole; 1-EtIm, 1-ethylimidazole; 2-MeHIm, 2-methylimidazole; 2-MeIm^-, 2-methylimidazolate.
6. Scheidt WR. J. Am. Chem. Soc 1974;96:84. [PubMed: 4810576]
7. (a) Stynes DV, Stynes HC, James BR, Ibers JA. J. Am. Chem. Soc 1973;95:1796. [PubMed: 4689919] (b) Stynes HC, Ibers JA. J. Am. Chem. Soc 1972;94:1559. [PubMed: 5015671]
8. (a) Collman JP, Gagne RR, Kouba J, Ljusberg-Wahren H. J. Am. Chem. Soc 1974;96:6800. [PubMed: 4414379] (b) Collman JP, Brauman JI, Doxsee KM, Halbert TR, Hayes SE, Suslick KS. J. Am. Chem. Soc 1978;100:2761. (c) Collman JP, Brauman JI, Doxsee KM, Halbert TR, Hayes SE, Suslick KS. Proc. Natl. Acad. Sci. U.S.A 1978;75:564. [PubMed: 273219]
9. Yamamoto K, Kwan T. J. Catal 1970;18:354.
10. Boulatov, R. N4-Macrocyclic Metal Complexes. Zagal, JH.; Bedioui, F.; Dodelet, J-P., editors. Vol. 1. Springer; New York: 2006. p. 1-36.
11. Shi C, Steiger B, Yuasa M, Anson FC. Inorg. Chem 1997;36:4294. [PubMed: 11670082]
12. Yoshimoto S, Inukai J, Tada A, Abe T, Morimoto T, Osuka A, Furuta H, Itaya K. J. Phys. Chem. B 2004;108:1948.
13. Collman JP, Gagne RR, Halbert TR, Lang G, Robinson WT. J. Am. Chem. Soc 1975;97:1427. [PubMed: 1133392]
14. Leggett, DJ. Computational Methods for the Determination of Formation Constants. Leggett, DJ., editor. Plenum; New York: 1985. Chapter 6
15. Sheldrick GM. Acta Chrystallogr 1990;A46:467.

16. Sheldrick, GM. Program for the Refinement of Crystal Structures. Universität Göttingen; Germany: p. 1997
17. $R_1 = \Sigma \parallel F_o| - |F_c \parallel / \Sigma |F_o|$ and $wR_2 = \{\Sigma[w(F_o^2 - F_c^2)^2]/\Sigma[wF_o^4]\}^{1/2}$. The conventional *R*-factors R_1 are based on *F*, with *F* set to zero for negative F^2. The criterion of $F^2 > 2\sigma(F^2)$ was used only for calculating R_1. *R*-factors based on F^2 (wR_2) are statistically about twice as large as those based on *F*, and *R*-factors based on ALL data will be even larger.
18. Sheldrick, GM. Program for empirical Absorption Correction of Area Detector Data. Universität Göttingen; Germany: p. 1996
19. Kitazawa T, Nishikiori S-I, Kuroda R, Iwamoto T. J. Chem. Soc., Dalton Trans 1994:1029. 1994.
20. Guerrero J, Piro OE, Wolcan E, Feliz MR, Ferraudi G, Moya SA. Organometallics 2001;20:2842.
21. Frost, AA.; Pearson, RG. Kinetics and Mechanism. John Wiley & Sons; New York: 1953. p. 28-31.Chapter 3
22. An introduction to NRVS is given in: Scheidt WR, Durbin SM, Sage JT. J. Inorg. Biochem 2005;99:60. [PubMed: 15598492]
23. Dwyer PN, Madura P, Scheidt WR. J. Am. Chem. Soc 1974;96:4815. [PubMed: 4854397]
24. Scheidt WR. J. Am. Chem. Soc 1974;96:90. [PubMed: 4810577]
25. Little RG, Ibers JA. J. Am. Chem. Soc 1974;96:4452. [PubMed: 4854396]
26. Jene PG, Ibers JA. Inorg. Chem 2000;39:5796. [PubMed: 11151382]
27. Jameson GB, Molinaro FS, Ibers JA, Collman JP, Brauman JI, Rose E, Suslick KS. J. Am. Chem. Soc 1980;102:3224.
28. Hu C, Roth A, Ellison MK, An J, Ellis CM, Schulz CE, Scheidt WR. J. Am. Chem. Soc 2005;127:5675. [PubMed: 15826208]
29. Ellison MK, Schulz CE, Scheidt WR. Inorg. Chem 2002;41:2173. [PubMed: 11952371]
30. Hu C, An J, Noll BC, Schulz CE, Scheidt WR. Inorg. Chem 2006;45:4177. [PubMed: 16676979]
31. Hoard JL, Scheidt WR. Proc. Natl. Acad. Sci. U.S.A 1973;70:3919. [PubMed: 4521218]
32. Hohenester E, Kratky C, Krautler B. J. Am. Chem. Soc 1991;113:4523.
33. Li, J-F.; Oliver, A.; Noll, BC.; Scheidt, WR. manuscript in preparation
34. Scheidt WR. J. Am. Chem. Soc 1974;96:84. [PubMed: 4810576]
35. Little RG, Ibers JA. J. Am. Chem. Soc 1974;96:4440. [PubMed: 4854394]
36. Lauher JW, Ibers JA. Inorg. Chem 1974;96:4447.
37. Bang H, Edwards JO, Kim J, Lawler RG, Reynolds K, Ryan WJ, Sweigart DA. Inorg. Chem 1992;114:2843.
38. Walker FA, Nasri H, Turowska-Tyrk H, Mohanrao K, Watson CT, Shokhirev NV, Debrunner PG, Scheidt WR. J. Am. Chem. Soc 1996;118:12109.
39. Hoard JL. Ann. N. Y. Acad. Sci 1973;206:18. [PubMed: 4518386]
40. Allen FH. Acta Crystallogr 2002;B58:380.Bruno IJ, Cole JC, Edgington PR, Kessler MC, Macrae F, McCabe P, Pearson J, Taylor R. Acta Crystallogr 2002:389.
41. Hu C, Noll BC, Piccoli PMB, Schultz AJ, Schulz CE, Scheidt WR. J. Am. Chem. Soc 2008;130:3127. [PubMed: 18271587]
42. Landrum JT, Hatano K, Scheidt WR, Reed CA. J. Am. Chem. Soc 1980;102:6729.
43. Freltag RA, Whitten DG. J. Phys. Chem 1983;87:3918.
44. Walker FA, Buehler J, West JT, Hinds JL. J. Am. Chem. Soc 1983;105:6923.
45. (a) Mazzanti M, Marchon J-C, Shang M, Scheidt WR, Jia S, Shelnutt JA. J. Am. Chem. Soc 1997;119:12400. (b) Veyrat M, Ramasseul R, Turowska-Tyrk I, Scheidt WR, Autret M, Kadish KM, Marchon J-C. Inorg. Chem 1999;38:1772. [PubMed: 11670946] (c) Song Y, Haddad RE, Jia S-L, Hok S, Olmstead MM, Nurco DJ, Schore NE, Zhang J, Ma J-G, Smith KM, Gazeau S, Pecaut J, Marchon J-C, Medforth CJ, Shelnutt JA. J. Am. Chem. Soc 2005;127:1179. [PubMed: 15669857]
46. Walker FA. J. Am. Chem. Soc 1973;95:1150. [PubMed: 4687684]
47. Stynes DV, Stynes HC, Ibers JA, James BR. J. Am. Chem. Soc 1973;95:1142. [PubMed: 4687683]
48. Dokuzovic Z, Ahmeti X, Pavlovic D, Murati I, Asperger S. Inorg. Chem 1982;21:1576.
49. Simplicio J, Wilkins RG. J. Am. Chem. Soc 1967;89:6092. [PubMed: 6066046]

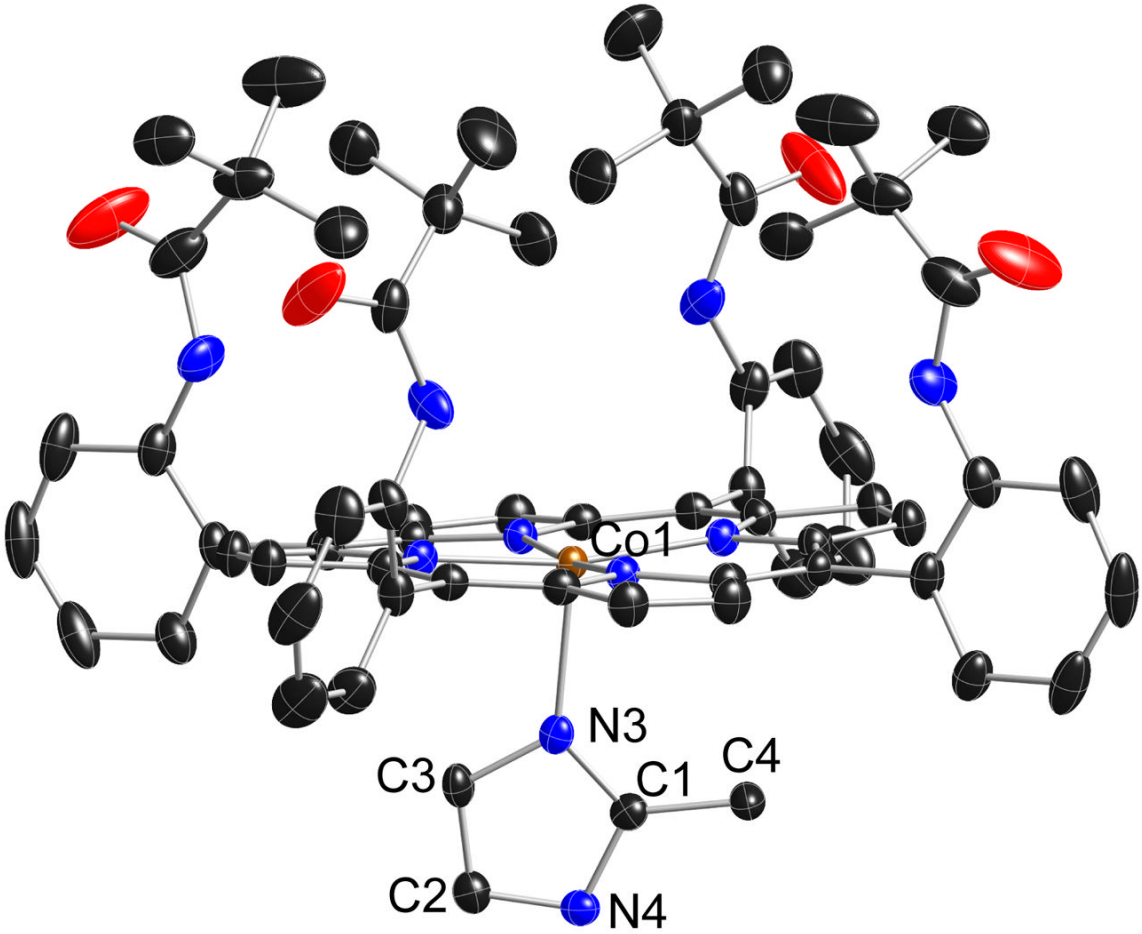

Figure 1.
Thermal ellipsoid plot of [Co(II)(TpivPP)(2-MeHIm)] displaying a partial atom labeling scheme. The molecule has a required twofold axis of symmetry perpendicular to the porphyrin plane. Thus the axial imidazole is disordered over two positions related by the required symmetry axis, but only one orientation is shown. Thermal ellipsoids of all atoms are contoured at the 50% probability level. Hydrogen atoms have been omitted for clarity.

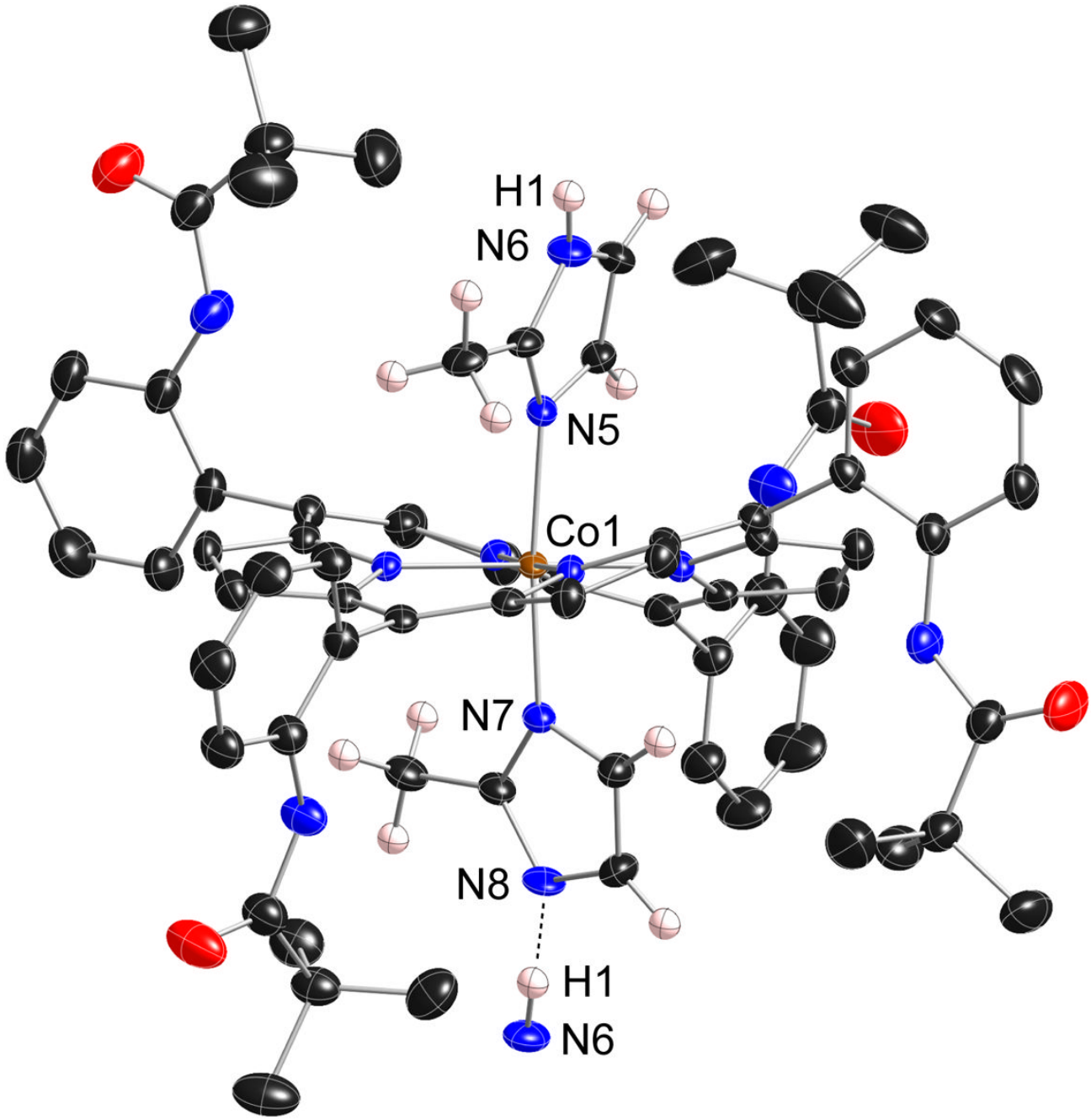

Figure 2.

Thermal ellipsoid diagram of [Co(*α*,*α*,*β*,*β*-TpivPP)(2-MeHIm)(2-MeIm^{-})](monoclinic) displaying the atom labels. The hydrogen atoms of the axial ligands are shown to display the hydrogen bond with the next molecule (N6···N8: 2.662(5)Å; N6···H1···N8: 171(6)°). Thermal ellipsoids of all atoms are contoured at the 50% probability level. Hydrogen atoms, except those of the imidazole ligands, have been omitted for clarity.

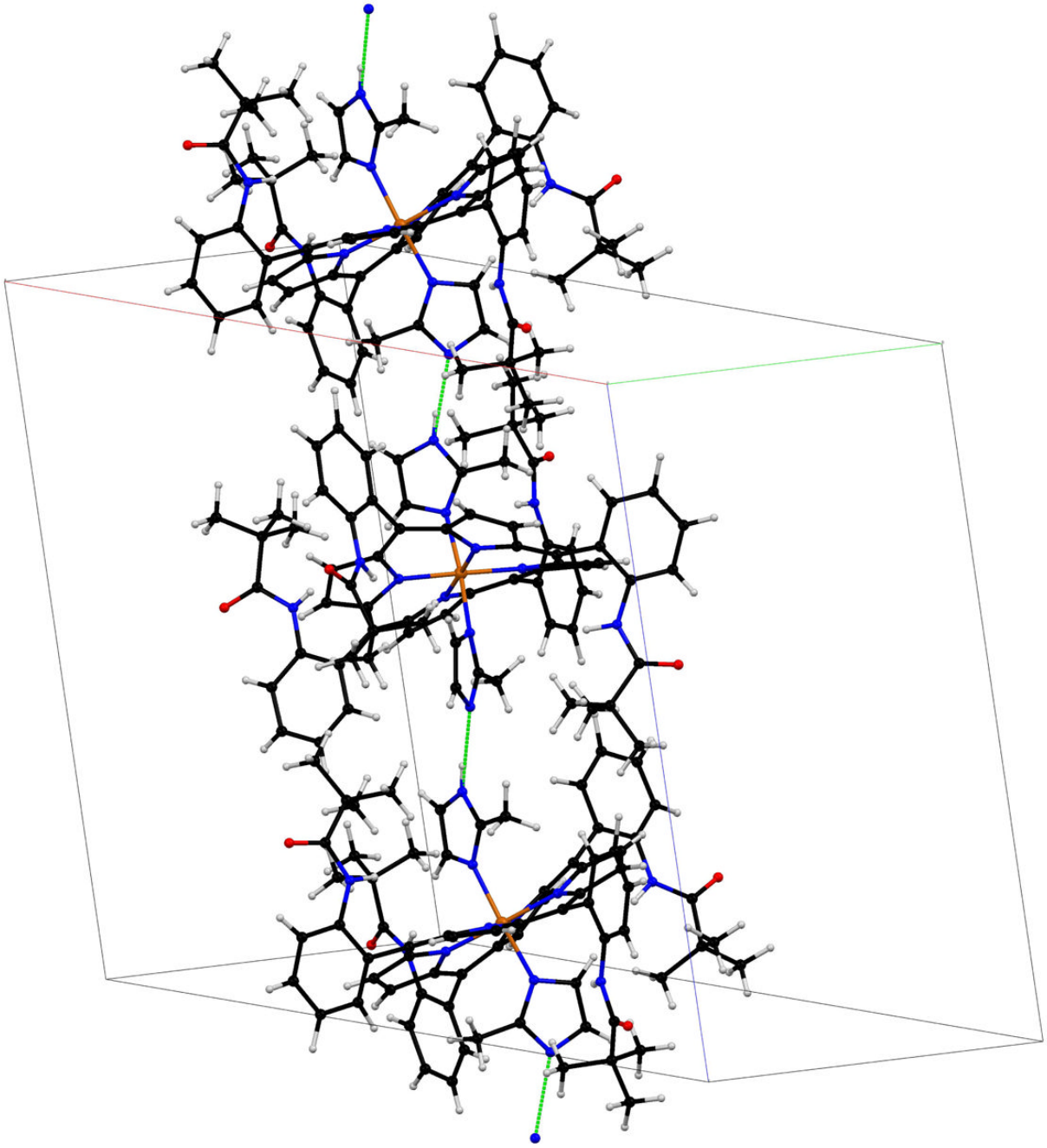

Figure 3.
Partial packing diagram of complex [Co(TpivPP)(2-MeHIm)(2-MeIm^{-})](monoclinic) showing the unit cell and the hydrogen bonds between the axial ligands. A second chain of opposite helicity exists in the complete crystal structure.

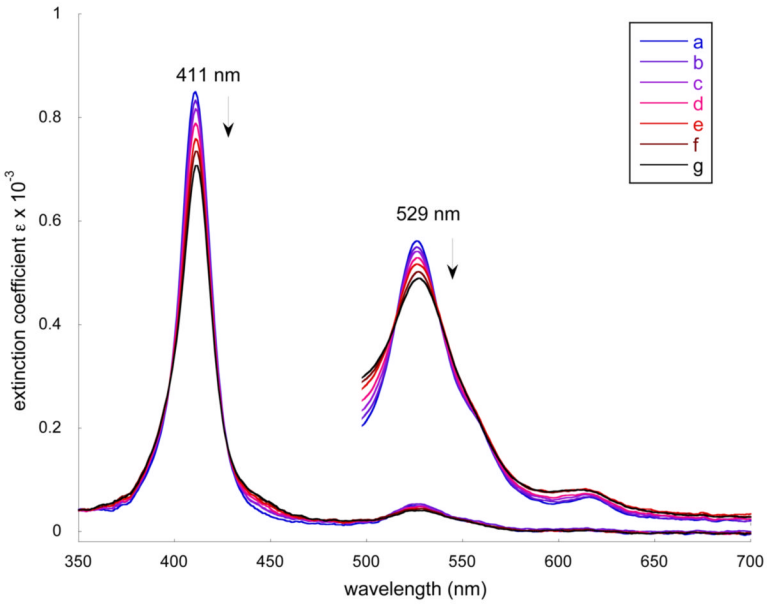

Figure 4.

Selected UV-vis spectra taken in benzene under argon. The enlarged spectra from 500 to 700 nm are measured in the 10-mm UV cell. a) [Co(II)(TpivPP)] (3.59×10^{-5} M) b) [Co(II)(TpivPP)] in 2.40×10^{-5} M 2-MeHIm solution. c) [Co(II)(TpivPP)] in 6.00×10^{-5} M 2-MeHIm solution. d) [Co(II)(TpivPP)] in 1.20×10^{-4} M 2-MeHIm solution. e) [Co(II)(TpivPP)] in 2.40×10^{-4} M 2-MeHIm solution. f) [Co(II)(TpivPP)] in 4.76×10^{-4} M 2-MeHIm solution. g) [Co(II)(TpivPP)] in 1.06×10^{-3} M 2-MeHIm solution.

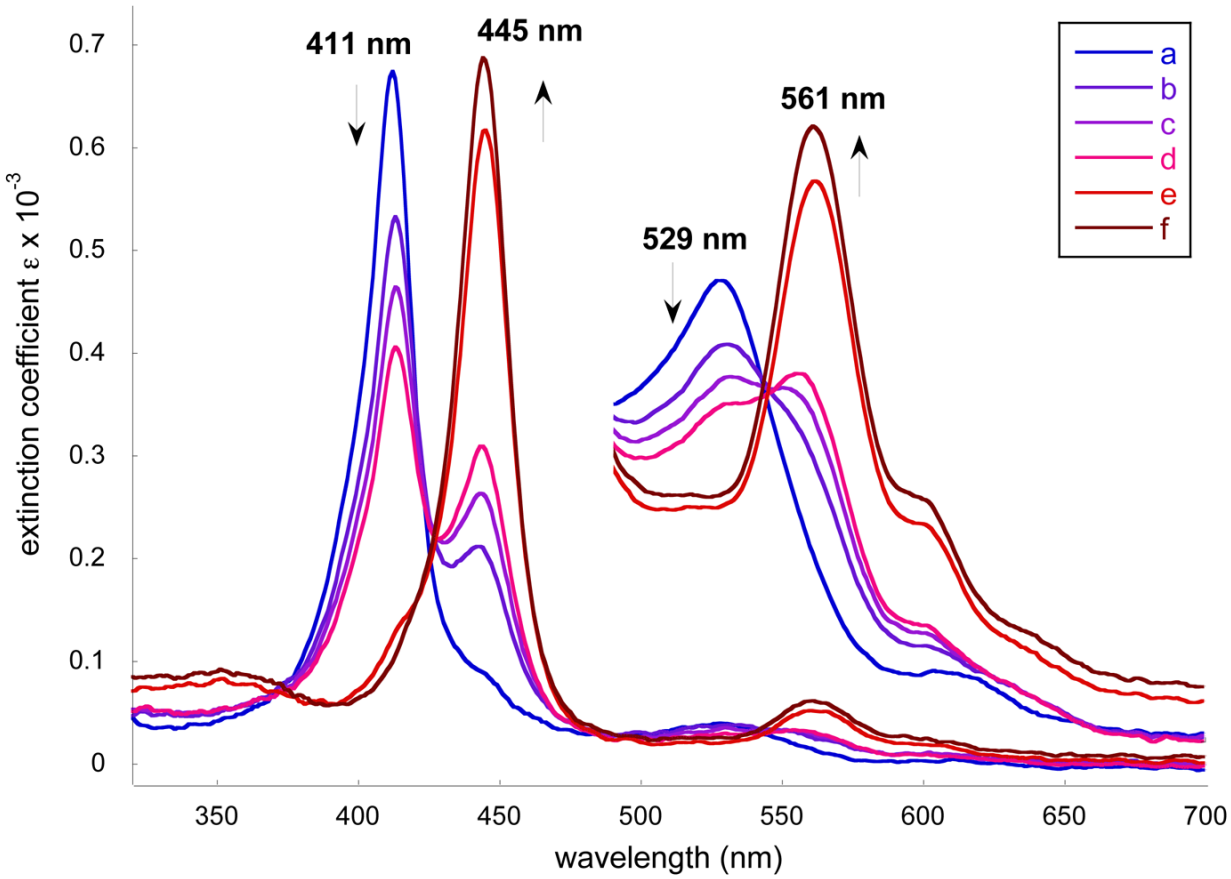

Figure 5.
Selected UV-vis spectra taken in benzene. a) [Co(II)(TpivPP)] (3.53×10^{-5} M) in 1.22×10^{-1} M 2-MeHIm solution. b) The solution was exposed to air for 15 mins. c) The solution was exposed to air for 30 mins. d) The solution was exposed to air for 40 mins. e) The solution was exposed to air for 5 hrs. f) The solution was exposed to air overnight.

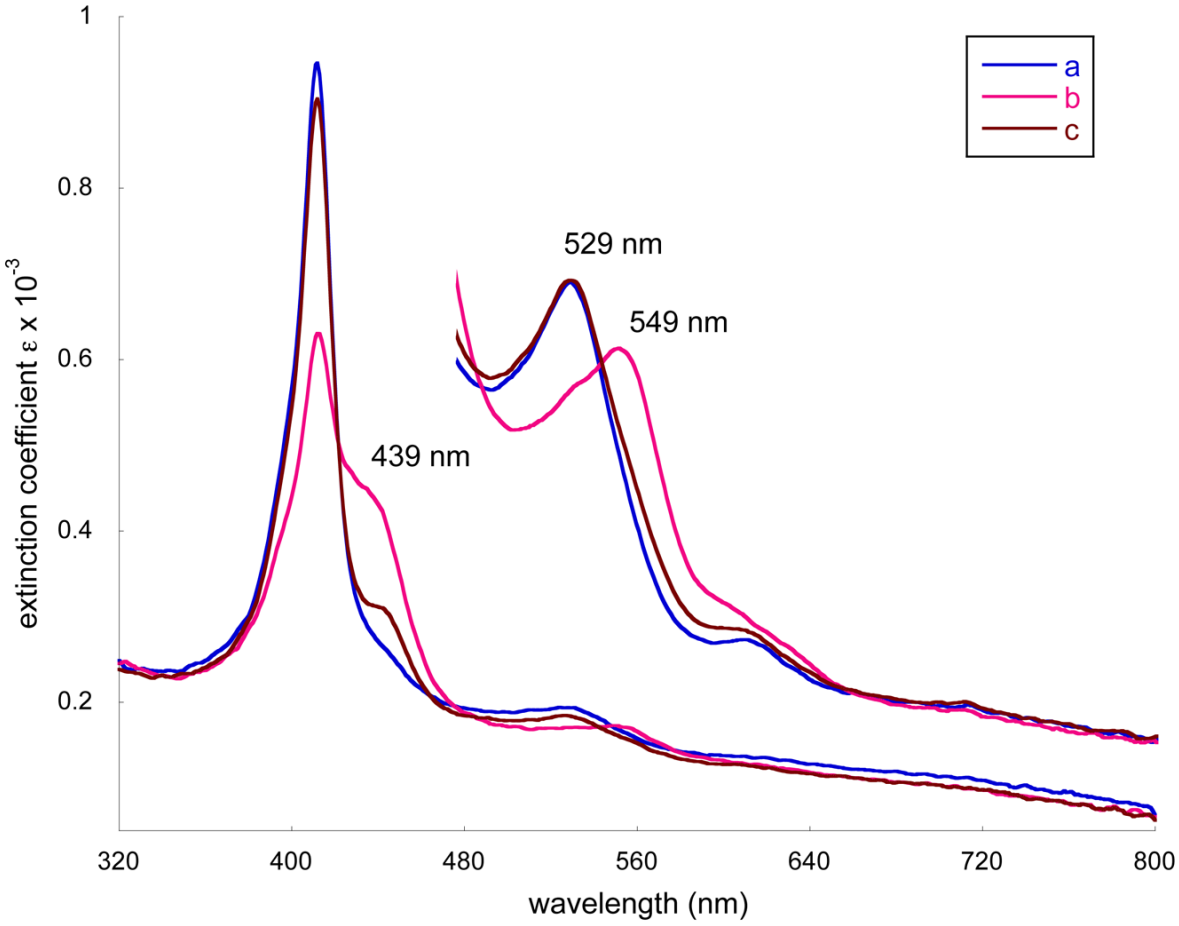

Figure 6.

Selected UV-vis spectra taken in benzene. The spectra from 480 to 800 nm are measured in the 10-mm UV cell. a) [Co(II)(TpivPP)] (3.59×10^{-5} M) in 5.97×10^{-3} M 2-MeHIm solution. b) Oxygen bubbled for 3 mins. c) Argon purge for 5 mins.

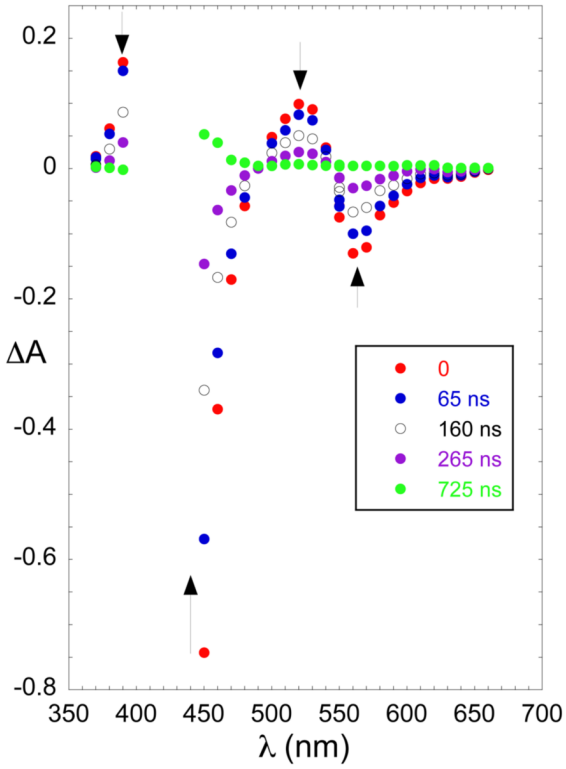

Figure 7.
Transient spectra recorded when an O_2 saturated solution of [Co(TpivPP)(2-MeHIm)] ([Co(TpivPP)] (3.59×10^{-5} M) in 2.80×10^{-3} M 2-MeHIm benzene solution) was irradiated at 351 nm. The delays from the laser flash are indicated in the figure.

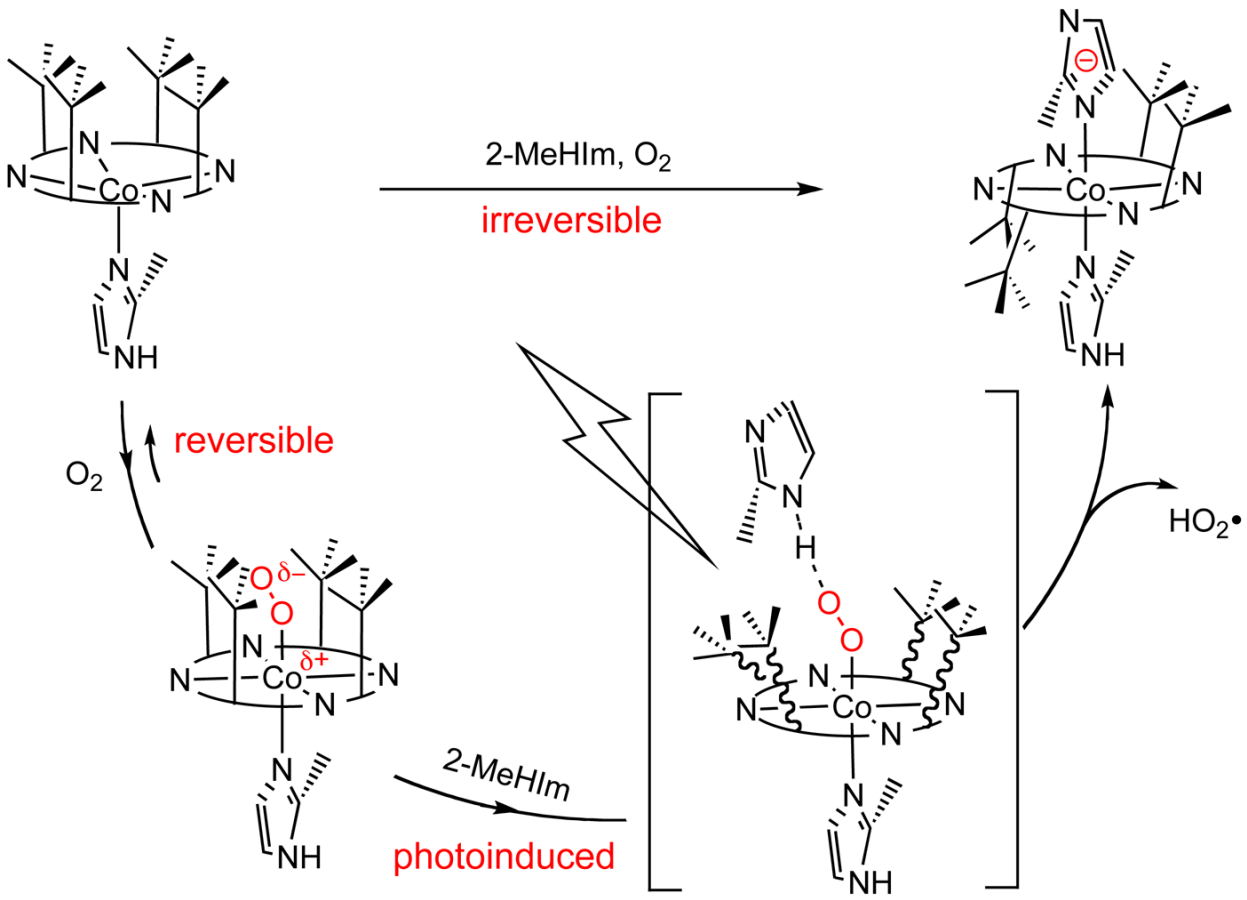

Scheme 1.
A proposed reaction route to the formation of [Co(III)(*α*,*α*,*β*,*β*-TpivPP)(2-MeHIm)(2-MeIm^{-})] from [Co(II)(TpivPP)(2-MeHIm)].

Table 1

Complete Crystallographic Details for [Co(TpivPP)(2-MeHIm)]·2C_2H_5OH, [Co(*α*,*α*,*β*,*β*-TpivPP)(2-MeHIm), (2-MeIm$^-$)](monoclinic), [Co(*α*,*α*,*β*,*β*-TpivPP)(2-MeHIm)(2-MeIm$^-$)] (triclinic)

	[Co(TpivPP)(2-MeHIm)] ·2C_2H_5OH	**[Co(*α*,*α*,*β*,*β*-TpivPP)(2-MeHIm) (2-MeIm$^-$)](monoclinic)**	**[Co(*α*,*α*,*β*,*β*-TpivPP)(2-MeHIm) (2-MeIm$^-$)](triclinic)**
chemical formula	$C_{72}H_{82}CoN_{10}O_6$	$C_{87.9}H_{90.9}CoN_{12}O_4$	$C_{79.05}H_{82.05}CoN_{12}O_4$
FW	1242.41	1438.36	1323.15
a, Å	18.5616(7)	24.4864(15)	13.6800(5)
b, Å	19.6540(7)	14.8242(9)	21.1364(7)
c, Å	17.8515(6)	21.1191(11)	26.2946(9)
α, deg	90	90	95.239(2)
β, deg	90.834(1)	104.159(2)	101.426(2)
γ, deg	90	90	102.866(1)
V, Å^3	6511.7(4)	7433.2(7)	7191.9(4)
space group	*C*2/*c*	$P2_1/c$	$P\bar{1}$
Z	4	4	4
temp, K	100	100	100
D_{calcd}, g cm^{-3}	1.267	1.285	1.222
μ, mm^{-1}	0.324	0.293	0.297
final *R* indices	R_1 = 0.0459	R_1 = 0.0769	R_1 = 0.0807
[I > 2*σ*(I)]	wR_2 = 0.1292	wR_2 = 0.1968	wR_2 = 0.2282
final *R* indices	R_1 = 0.0593	R_1 = 0.1015	R_1 = 0.1192
(all data)	wR_2 = 0.1400	wR_2 = 0.2146	wR_2 = 0.2597

Table 2

Selected Structural Parameters for Five-Coordinate [Co(II)(Por) (RIm)] and Related Iron(II) Species [a]

Complex	Δ_{24} [b]	$(M–N_p)_{av}$	$M–N_{im}$ [c]	ϕ_{im} [d]	ref.
		Co(II) complexes			
[Co(II)(TpivPP)(2-MeHIm)]	0.15	1.979(3)	2.145(3)	21.6	tw
[Co(II)(TPP)(l,2-Me_2Im)]	0.18	1.985(3)	2.216(2)	20.0	23
[Co(II)(TPP)(1-MeIm)]	0.13	1.977(6)	2.157(3)	4.1	24
[Co(II)(OEP)(1-MeIm)]	0.16	1.96(1)	2.15(1)	10	25
[Co(II)(OC_3OP)(1-MeIm)]	0.13	1.985(6)	2.132(3)	15.6	26
		Fe(II) complexes			
[Fe(II)(TpivPP)(2-MeHIm)]	0.43	2.072(6)	2.095(6)	22.8	27
[Fe(II)(TPP)(1,2-Me_2Im)]	0.42	2.079(8)	2.158(2)	20.9	28
[Fe(II)(TTP)(2-MeHIm)]	0.39	2.076(3)	2.144(1)	35.8	28
[Fe(II)(T_p-OCH_3PP)(2-MeHIm)]	0.51	2.087(7)	2.155(2)	44.5	28
[Fe(II)(T_p-OCH_3PP)(1,2-Me_2Im)]	0.38	2.077(6)	2.137(4)	20.7	28
[Fe(II)(TPP)(2-MeHIm)]·1.5C_6H_5Cl	0.38	2.073(9)	2.127(3)	24.0	29
[Fe(II)(OEP)(l,2-Me_2Im)]	0.45	2.080(6)	2.171(3)	10.5	30
[Fe(II)(OEP)(2-MeHIm)]	0.46	2.077(7))	2.135(3)	19.5	30

[a] Distances in Å, Angles in deg., tw = this work.

[b] Displacement of the metal atom from the 24-atom mean plane, a positive number indicates a displacement toward the imidazole ligand.

[c] Bond distance between iron atom and imidazole nitrogen atom.

[d] Dihedral angle between the planes defined by the closest N_p–M–N_{im} and the imidazole plane.

Table 3

Selected Structural Parameters of Six-coordinate [Co(Por)(L)$_2$] Complexes[a]

Complex	Δ_{24}[b]	(Co–N$_p$)$_{av}$	Co–L$_{fifth}$[c]	Co-L$_{Sixth}$[d]	ϕ_{fifth}[e]	ϕ_{sixth}[e]	θ[f]	ref.
Co(II) complexes								
[Co(II)(TPP)(pip)$_2$] (2-fold)	0.00	1.987(2)	2.436(2)	2.436(2)	–	–	–	34
[Co(II)(OEP)(3-MePy)$_2$] (2-fold)	0.00	1.992(1)	2.386(2)	2.386(2)	12.03	12.03	0.00	35
Co(III) complexes								
[Co(III)($\alpha,\alpha,\beta,\beta$-TpivPP)(2-MeHIm)(2-MeIm$^-$)]	0.00	1.934(5)	1.972(3)	1.953(3)	43.4	34.3	80.2	tw
[Co(III)($\alpha,\alpha,\beta,\beta$-TpivPP)(2-MeHIm)(2-MeIm$^-$)] (mol 1)	−0.03	1.943(5)	1.972(3)	1.957(3)	36.6	33.1	71.2	tw
[Co(III)($\alpha,\alpha,\beta,\beta$-TpivPP)(2-MeHIm)(2-MeIm$^-$)] (mol 2)	0.05	1.951(4)	1.957(3)	1.952(3)	37.7	44.4	85.7	tw
[Co(III)(TPP)(HIm)$_2$]OAc [g]	0.00	1.982(11)	1.945(15)	1.945(15)	43	43	0	36
[Co(III)(TDCPP)(1-MeIm)$_2$]BF$_4$	0.01	1.977(5)	1.942(5)	1.941(6)	11.2	10.0	89.8	37

[a] Distances in Å, Angles in deg., tw = this work.

[b] Displacement of the metal atom from the 24-atom mean plane, a positive number indicates a displacement toward the imidazole ligand.

[c] Bond distance between iron atom and imidazole (pip, Py) nitrogen atom.

[d] Bond distance between iron atom and the coordinate atom of sixth ligand.

[e] Dihedral angle between the planes defined by the closest N$_p$–Co–N$_{im/im-}$ and the imidazole or imidazolate plane.

[f] Dihedral angle between the planes defined by two axial ligand planes.

[g] The data is cited for one of the two half-porphyrins in the asymmetric unit.